Scalable nano-particle assembly by efficient light-induced concentration and fusion

Benjamin K. Wilson[1], Mike Hegg[1], Xiaoyu Miao[1], Guozhong Cao[2] and Lih Y. Lin[1,3]

[1]*Department of Electrical Engineering, University of Washington, Seattle, Washington 98195, USA*
[2]*Department of Material Science and Engineering, University of Washington, Seattle, Washington 98195, USA*
[3]*Department of Physics, University of Washington, Seattle, Washington 98195, USA*
[*]*Corresponding author: bewsilon@u.washington.edu*

Abstract: Avalanche concentration, a rapid, long-range accumulation of particles around a laser spot in a liquid sample, is demonstrated and characterized for various nanoparticles (NPs). The effect is driven by a convective flow in the sample, caused by efficient heating of NPs with high absorption efficiencies. Several types of concentration behavior were observed and characterized. Control of optical power and initial particle density was found to be effective in determining the assembly process. VO_2 nanowires, carbon nanotube (CNT), and quantum dot (QD) electrode gap bridges were assembled with a variety of sizes and geometries to show the utility of the method for nano-assembly. Bridges were assembled from as many as thousands to as few as one NP and were found to form solid electrical contact between the electrodes, as verified by measuring the current - voltage (I-V) characteristic.

OCIS codes: (350.4855) Optical manipulation

References and links

1. R. Krupke, F. Hennrich, H. B. Weber, M. M. Kappes, and H. v. Lohneysen, "Simultaneous deposition of metallic bundles of single-walled carbon nanotubes using AC-dielectrophoresis," Nano Lett. **3**, 1019-1023 (2003).
2. L. Dong, V. Chirayos, J. Bush, J. Jiao, V. M. Dubin, R. V. Chebian, Y. Ono, J. John F. Conley, and B. D. Ulrich, "Floating-potential dielectrophoresis-controlled fabrication of single-carbon-nanotube transistors and their electrical properties," J. Phys. Chem. B **109**, 13148-13153 (2005).
3. P. J. Pauzauskie, A. Radenovic, E. Trepagnier, H. Shroff, P. Yang, and J. Liphardt, "Optical trapping and integration of semiconductor nanowire assemblies in water," Nat. Mater. **5**, 97-101 (2006).
4. J. M. Tour, L. Cheng, D. P. Nackashi, Y. Yao, A. K. Flatt, S. K. S. Angelo, T. E. Mallouk, and P. D. Franzon, "Nanocell electronic memories," J. Am. Chem. Soc. **125**, 13279-13283 (2003).
5. G. Konstantatos, I. Howard, A. Fischer, S. Hoogland, J. Clifford, E. Klem, L. Levina, and E. H. Sargent, "Ultrasensitive solution-cast quantum dot photodetectors," Nature **442**, 180-183 (2006).
6. J. Liu, and Y. Lu, "A colorimetric lead biosensor using DNAzyme-directed assembly of gold nanoparticles" J. Am. Chem. Soc. **125**, 6642 (2003).
7. S. Y. Park, A. K. R. Lytton-Jean, B. Lee, S. Weigand, G. C. Schatz, and C. A. Mirkin, "DNA-programmable nanoparticle crystallization," Nature **451**, 553-556 (2008).
8. S. Y. Park, J.-S. Lee, D. Georganopoulou, C. A. Mirkin, and G. C. Schatz, "Structures of DNA-Linked Nanoparticle Aggregates," J. Phys. Chem. B **110**, 12673-12681 (2006).
9. V. Garcés-Chávez, R. Quidant, P. J. Reece, G. Badenes, L. Torner, and K. Dholakia, "Extended organization of colloidal microparticles by surface plasmon polariton excitation," Phys. Rev. B **73**, 085417 (2006).
10. K. C. Toussaint, M. Liu, M. Pelton, J. Pesic, M. J. Guffey, P. Guyot-Sionnest, and N. F. Scherer, "Plasmon resonance-based optical trapping of single and multiple Au nanoparticles," Opt. Express **15**, 12017-12029 (2007).
11. S. Duhr, and D. Braun, "Two-dimensional colloidal crystals formed by thermophoresis and convection" Appl. Phys. Lett. **86**, 131921 (2005).
12. D. P. O'Neala, L. R. Hirschb, N. J. Halasc, J. D. Paynea, and J. L. Westb, "Photo-thermal tumor ablation in mice using near infrared-absorbing nanoparticles," Cancer Lett. **209**, 171-176 (2004).
13. A. Ashkin, J. M. Dziedzic, J. E. Bjorkholm, and S. Chu, "Observation of a single-beam gradient force optical trap for dielectric particles," Opt. Lett. **11**, 288-290 (1986).

#100256 - $15.00 USD Received 18 Aug 2008; revised 1 Oct 2008; accepted 4 Oct 2008; published 13 Oct 2008

14. A. S. Zelenina, R. Quidant, and M. Nieto-Vesperinas, "Enhanced optical forces between coupled resonant metal nanoparticles," Opt. Lett. **32** (2007).
15. M. Eagleson, *Concise Encyclopedia Chemistry* (Walter de Gruyter, 1994).
16. W. A. Goddard, D. W. Brenner, and S. E. Lyshevski, *Handbook of Nanoscience, Engineering, and Technology* (CRC Press, 2002).
17. H. Kakiuchida, P. Jin, S. Nakao, and M. Tazawa, "Optical properties of vanadium dioxide film during semiconductive-metallic phase transition," Jpn. J. Appl. Phys. **46**, L113–L116 (2007).

1. Introduction

Nanoparticle (NP) assembly has been a topic of great interest in recent years. This is first due to the unique physical properties of NPs such as carbon nanotubes, quantum dots, and metal oxide nanorods and their potential for use in novel devices such as sensors and circuit elements. In addition, novel nano-assembly methods are vital to the implementation of such devices due to the NPs incompatibility with conventional IC fabrication processes. Liquid-phase deposition has been realized using AC dielectrophoresis with CNTs [1, 2]. These processes generally aim to align a single CNT between two electrodes. More recently, optical trapping has been used to assemble semiconductor nanowires in liquid solution [3]. These methods are generally used to precisely aligning a small number of NPs.

In addition to the unique properties of single NPs, it has been shown that larger systems of NPs can achieve unique functions such as improved conductivity interconnects, biological sensors, optical sensors and photovoltaics, and electronic gate and memory devices [1, 4-6]. Larger scale assembly of NPs has generally been realized using chemical methods [7, 8]. Among these, assembly in solution has been realized by optical methods in several instances. These include ordered and disordered structures formed using surface plasmon polariton excitation [9, 10], and convective flow with thermophoresis [11]. In this paper we explore a new method of forming and precisely placing NP assemblies from nano-particles in solution.

2. Operating principle and modeling

The avalanche concentration process utilizes two main forces, the drag from the convective flow of the liquid induced by a localized temperature gradient and the optical forces caused by the focused Gaussian optical beam (Figure 1). When NPs with large absorption cross-sections are excited by optical radiation, they can produce large amounts of heat due to enhanced absorption. This process has been well characterized for gold NPs for use in biological applications [12]. In our NP assembling experiments, the highly absorbing NPs are VO_2 nanorods, multi-walled CNTs, and CdTe QDs in solution. The high absorption efficiency of the NPs generates heat and elevates the temperature of the surrounding liquid. This produces a localized temperature gradient which causes a convective flow to form in the solution. The convective flow was modeled using FEMLAB to solve both the incompressible Navier-Stokes equation and the combined conduction-convection heat transfer equation. The absorption of the NPs under laser excitation was modeled as a heat flux source with Gaussian distribution close to the no-slip lower boundary between water and glass. As shown in Figure 1a, the steady-state flow pulls in colder liquid from along the bottom of the sample and pushes it upward into the solution.

In addition to the convective flow, there are multiple optical forces which have much shorter range. First is the gradient force, the driving force of optical tweezers, which acts to pull the particle into the region of highest optical intensity of the Gaussian beam. There is also the scattering force, which pushes the particle in the direction of light propagation. These forces have been well characterized [13] and will not be described here. To model the interaction of the optical forces with the drag from convective flow, optical forces were approximated for a weakly focused Gaussian beam acting on a dielectric sphere, namely $\mathbf{F}_{Grad} \propto \nabla I(\mathbf{r})$ and $\mathbf{F}_{Scat} \propto \mathbf{k} I(\mathbf{r})$, where $\mathbf{F}_{Grad}$ and $\mathbf{F}_{Scat}$ are the gradient and scattering force vectors, respectively, $I(\mathbf{r})$ is the optical intensity and $\mathbf{k}$ is the unit wave vector. Fig. 1(b) shows the expected trajectory of a NP near a Gaussian beam with a 10 μm beam diameter

#100256 - $15.00 USD Received 18 Aug 2008; revised 1 Oct 2008; accepted 4 Oct 2008; published 13 Oct 2008

considering both optical forces and convective flow. Blue lines indicate trajectories where the convective flow dominates the optical forces, while orange lines indicate the optical forces dominating convective flow.

In addition to the gradient and scattering forces, other optical forces can be observed in the system. As will be shown in the experimental results for VO_2 nanorods (Fig. 2(d)), the NPs remain trapped well outside of the optical beam spot, and therefore outside the range of both the gradient and scattering forces. One likely explanation is a form of enhanced optical binding force between the nanorods [14] through plasmonic effects.

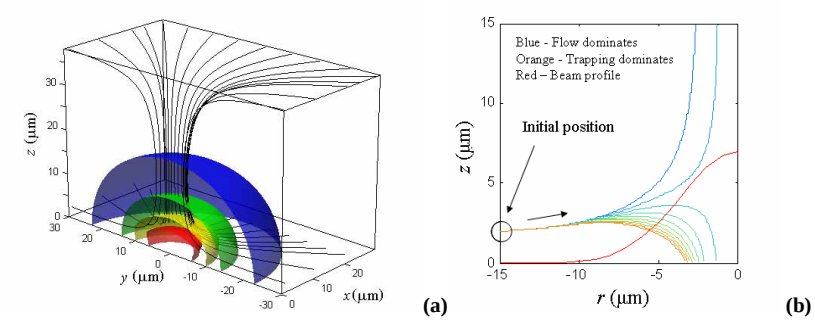

Fig. 1. (a) FEMLAB simulation of convective flow caused by a Gaussian-distributed heat source along a glass-water interface located at the z = 0 plane, colors show change in temperature (blue 5 degree kelvin, green 10K, yellow 15K, red 20K) and streamlines show fluid velocity. (b) Simulated trajectories for a NP with combined effects from the convective flow, optical scattering force and gradient force.

3. Controlled concentration of VO_2 nanorods

To demonstrate controlled avalanche concentration, VO_2 nanorods were used with TiO_2 NPs as a control. The VO_2 nanorods ranged from 2-15 μm in length with a diameter of 150 to 250 nm. The control TiO_2 NPs were at anatase phase, about 2 μm in diameter, roughly shaped, with an aspect ratio less than 1:1.3. Samples with several concentrations of NPs in water were prepared. The solutions were placed on a glass slide, with glass spacers and coverslip. A 25mW 633nm HeNe laser was used as the excitation source focused by a 20x objective lens with a low numerical aperture (N.A.) of 0.22, producing a spot diameter of 10 μm. The laser power measured on the sample could be adjusted from 0 to 5 mW using a neutral density attenuator. Tests were performed with NPs that had settled onto the water-glass interface.

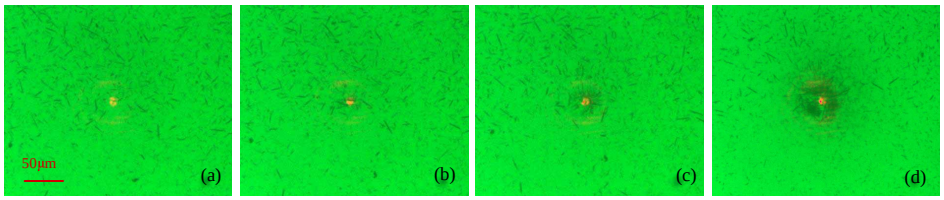

Fig. 2. Avalanche concentration with VO_2 nanorods. (a) Laser excitation is initiated, at first nothing happens until a nanorod enters the spot by optical trapping or brownian motion. (b) Convective flow begins and nanorods adjacent to the spot are pulled in (2 seconds). (c) Avalanche clustering reaches full strength as the laser spot is filled with nanorods. Convective flow pulls in nanorods from over 150 μm away (5 seconds). (d) System reaches steady-state as accumulation around the spot disrupts the convective flow and the process stops (30 seconds).

The concentration results differed based on the NP material, the incident power, and the initial density of the NPs. For TiO_2, no concentration was observed at any configuration of the latter two parameters. This was presumably because TiO_2 has minimal absorption efficiency at 633 nm wavelength. Therefore, very little optical energy was transferred to heat and no convective flow was formed. For VO_2, once at least one NP entered a laser spot of

#100256 - $15.00 USD Received 18 Aug 2008; revised 1 Oct 2008; accepted 4 Oct 2008; published 13 Oct 2008

sufficient intensity a weak convective flow was formed, pulling other adjacent nanorods into the laser spot (Fig. 2(a) and 2(b)). As more NPs were concentrated at the laser spot, the absorption increased, thus increasing the heat and the convective flow, pulling in even more NPs. This positive feedback system led to an avalanche effect, where a very strong convective flow was formed within seconds, pulling in particles from more than 200 μm away (Fig. 2(c)).

Once the convective flow was formed, several different behaviors were observed. For VO_2 nanorods, similar system behaviors were classified into regions defined by incident power and mean initial separation distance of the nanorods (see Fig. 3). The system behaviors could be explained by the interplay of the forces present in the system. For low to mid-range incident powers and mid-range mean separations, stable concentration was observed. In this regime, a convective flow was established as described above and continued until the area around the light spot was saturated with nanorods. This saturation blocked the inward flowing water from reaching the laser spot and the convective flow stopped. This is the result shown in Fig. 2(d) (corresponding to P = 2mW and d = 8.5μm in Fig. 3). Stable trapping was enabled by the optical forces dominating the convective flow at the final state (see Fig. 1(b)).

At the highest incident powers and lowest mean particle separations the process became unstable. In this regime, the effect of convective flow is significantly larger than the optical forces. The convective flow became very strong, to the point that it swept the nanorods through the laser spot region without being trapped by the optical forces (See Fig. 1(b)). Between the stable and unstable trapping regions was a region of metastable concentration in which characteristics of both stable and unstable processes were observed.

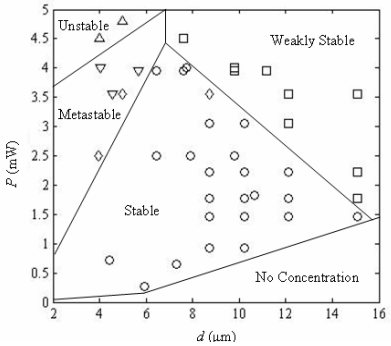

Fig. 3. Stability diagram for avalanche concentration with VO_2 nanorods versus mean initial particle separation (d) and incident power (P). Stable concentration is represented by circles, metastable – diamonds and down pointing triangle, unstable – up pointing triangle, weakly stable – squares.

The final behavior, observed in VO_2 nanorod solutions with high incident powers and large mean separations, was weakly stable concentration. In this regime, adjacent nanorods were pulled into the laser spot area but no long-range convective flow was formed. This was due to the scattering force repelling the rods from the center of the spot, causing adjacent nanorods to form a loose ring around the spot (this repulsion was not observed with TiO_2 NPs). With only small amounts of the rods in the spot, not enough heat was generated to form the previously described positive feedback. This repulsive scattering force was also observed in stable concentration as is clearly visible in Fig. 2(d). All avalanche concentration processes were observed to be reversible – rods that were concentrated quickly disperse back into the solution when the laser was turned off. The processes were found to be repeatable as well.

4. Assembling of NPs

To demonstrate large-scale assembly of NPs using the avalanche concentration process, electrode gap bridges were fabricated from a variety of absorbing NPs. The previously mentioned optical setup was used, only without a cover slip to allow the solution to evaporate.

#100256 - $15.00 USD Received 18 Aug 2008; revised 1 Oct 2008; accepted 4 Oct 2008; published 13 Oct 2008

It was found that adding isopropyl alcohol (IPA) to the solution served to both decrease the solution viscosity, leading to better mixed and dispersed NPs, and increase the rate of evaporation. As the IPA evaporated before the water, the IPA did not affect the final stages of assembly. In place of a glass substrate a Si/SiO_2 substrate with patterned gold electrodes was used.

Utilizing the described process a variety of electrode gap bridges was assembled (Fig. 4). The process was found to be most rapid in the final stages of evaporation, with decreased liquid volume and formation of a stronger convective flow. Once the avalanche concentration process was initiated, the laser spot was slowly moved across the electrode gap. Concentrated NPs adhered to the gold electrodes. The low power laser light was found to generate sufficient heat to melt the NPs due to their high absorption and the vanishing liquid volume, allowing the laser spot to be used as a type of pen, drawing an arbitrary shape of fused NPs.

Unlike in bulk solution, when liquid volumes were low the avalanche concentration was no longer a reversible process. Assemblies of NPs did not disperse after the laser was turned off. Observation under SEM showed two ways in which NPs were kept from diffusing, presumably dependent on the generated heat. As shown in Figure 4, in lower temperature situations (lower laser power, fewer NPs) the individual NPs maintained their shape but appeared fused together (Fig. 4(c)). In higher temperature situations (higher power, more NPs) they appeared to melt into a solid block (Fig. 4(e)). This was unexpected, considering the melting temperature of VO_2 is 1967ºC [15] and CNTs is >2000ºC [16].

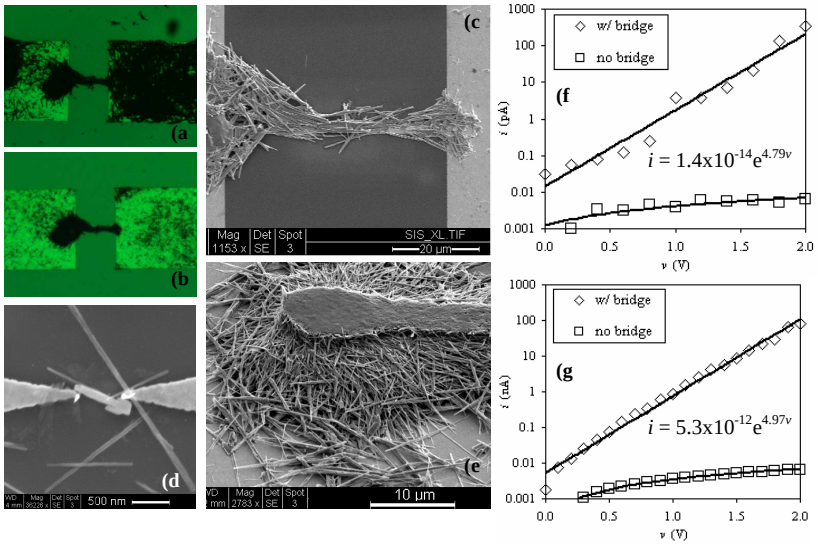

Fig. 4. Optical microscopy images of an assembled VO_2 bridge pre-rinse (a), and post-rinse(b). (c) SEM image of same bridge showing fused nanorods. (d) SEM image of a single nanorod aligned and fused between two electrodes. (e) SEM image of a melted VO_2 cluster. I-V plots for a single nanorod bridge (f) and a bridge containing about 100 nanorods (g).

After evaporation, annealing was used to strengthen the bridges by assuring the NPs were fused together and to the substrate. This was done by slowly passing the laser spot over the bridge, thus further heating the NPs. After annealing, the samples were ultrasonicated in acetone and rinsed in IPA and water to help remove undesired NPs deposited on the substrate. In most cases only the annealed sections of the sample remained after rinsing (Fig. 4(a) and 4(b)). Using this method NP electrode bridges were assembled composed of thousands of NP (Fig. 4(c)) or as few as one (Fig. 4(d)).

VO_2 nanorods were found to be easier manipulated using this process than CNTs. The rigid shape and size of the VO_2 nanorods was ideal for producing assemblies with highly

#100256 - $15.00 USD Received 18 Aug 2008; revised 1 Oct 2008; accepted 4 Oct 2008; published 13 Oct 2008

controllable sizes and shapes. CNTs assembled very efficiently but were much less controllable, mostly due to their non-rigid form, causing the final assemblies to be tangled bundles of CNTs. Despite this, CNT assemblies could still be produced with very repeatable sizes and precise positioning (see Fig. 5(a)). QDs were also found to efficiently assemble, however the assemblies were unstable and tended to break apart, most likely due to lack of adhesive forces between the QDs (Fig. 5(b)).

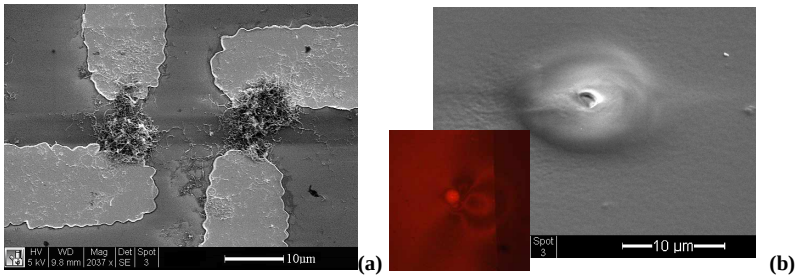

Fig . 5. (a) SEM of an assembled CNT bridge showing fused NPs. (b) SEM image of a cluster of CdTe QDs assembled using avalanche concentration. (inset) Fluorescence image of same QD cluster.

Finally to confirm that the VO_2 and CNT bridges successfully contacted the electrodes and form good conduction paths, the I-V characteristics of the electrodes with and without bridges were compared (see Fig. 4(f) and 4(g)). The electrodes bridged with any number of VO_2 nanorods were found to have an exponential current to voltage relationship. This implies that tunneling plays a role in conduction between the electrode or perhaps a heat driven insulator-metal transition is occurring in the VO_2 nanorods [17]. The single-rod bridge also shows good conduction, although the current through the device was found to fluctuate as much as an order of magnitude over time under a constant voltage bias. This fluctuation was possibly due to the conduction path changing as the single rod changed phase with changing temperature. Larger bridges were found to have much larger and more stable currents. CNT bridges showed linear I-V characteristics with much higher currents than VO_2. A bridge containing approximately 100 CNTs had a measurable resistance of 60 Ω. The open electrodes had a linear current to voltage relationship with currents several orders of magnitude below the bridged gaps (Fig. 4(f) and 4(g)).

5. Conclusion

We have demonstrated a new opto-fluidic phenomenon which we call avalanche concentration. This method was used to concentrate large assemblies of absorbing NPs with high controllability and requires only a microscope with a weakly-focused, low-power laser beam. It has also been shown that by controlling the process and micro-fluidic condition, avalanche concentration is capable of assembling electrode gap bridges using a variety of nano-particles. These bridges have been found to be stably fused and well contacted to the electrodes. Due to its ability to assemble NP structures of arbitrary shape over a wide range of sizes, avalanche concentration may find many potential applications involving assembling NPs across the field of nanotechnology.

Acknowledgments

This work has been supported by the National Science Foundation (DBI 0454324) and the National Institutes of Health (R21 EB005183). Imaging of the fabrication results was performed in part at the University of Washington Nanotech User Facility (NTUF), a member of the National Nanotechnology Infrastructure Network (NNIN), which is supported by the National Science Foundation.

#100256 - $15.00 USD Received 18 Aug 2008; revised 1 Oct 2008; accepted 4 Oct 2008; published 13 Oct 2008